JOC The Journal of Organic Chemistry

Article

pubs.acs.org/joc

Aromaticity Competition in Differentially Fused Borepin-Containing Polycyclic Aromatics

Reid E. Messersmith,[†] Maxime A. Siegler,[†] and John D. Tovar*[,†,‡]

[†]Department of Chemistry and [‡]Department of Materials Science and Engineering, Johns Hopkins University, 3400 North Charles Street, Baltimore, Maryland 21218, United States

Supporting Information

ABSTRACT: This report describes the synthesis and characterization of a series of borepin-based polycyclic aromatics bearing two different arene fusions. The borepin synthesis features streamlined Ti-mediated alkyne reduction, leading to *Z*-olefins, followed by direct lithiation and borepin formation. These molecules allow for an assessment of aromatic competition between the fused rings and the central borepin core. Crystallographic, magnetic, and computational studies yielded insights about the aromaticity of novel, differentially fused [*b*,*f*]borepins and allowed for comparison to literature compounds. Multiple borepin motifs were also incorporated into polycyclic aromatics with five or six rings in the main backbone, and their properties were also evaluated.

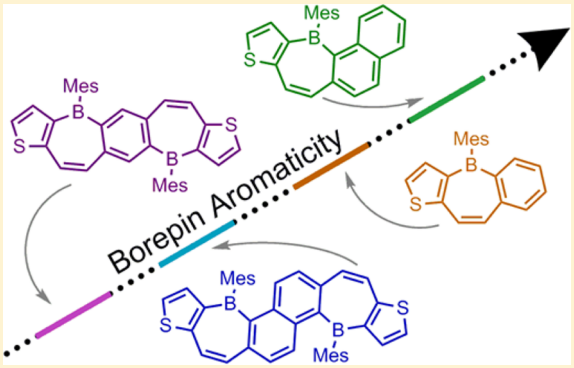

INTRODUCTION

Borepins are seven-membered ring systems with 6 π-electrons that attract attention because of their weak, nonbenzenoid aromatic character.[1−3] The boron atom is less electronegative than the surrounding carbon atoms and also has an empty p-orbital available for π-conjugation.[4,5] Computational and experimental studies reveal that boron-bound atoms with lone pairs,[6,7] external η^7-coordination,[8] attachment of electron donating/withdrawing groups,[9] or even competing aromatic ring systems[10] fused to the borepin periphery can greatly modulate the aromaticity of the borepin ring. The boron atom within the heteroaromatic ring typically requires a steric blocking group to protect the vacant p-orbital from nucleophilic attack.[2,11] Polycyclic aromatics that incorporate borepin rings have shown air, water, and chromatographic stability due to kinetic protecting groups and π-electron donation from neighboring systems. Mercier et al. reported dibenzo[*b*,*f*]-borepin (**1a**), benzonaphtho[*b*,*f*]borepin (**2**), and dinaphtho-[*b*,*f*]borepin (**3**) with *B*-mesityl groups (2,4,6-trimethylphenyl, Mes) to add kinetic protection for the empty p-orbital on the boron.[12] Our group reported supermesityl (2,4,6-tri-*t*-butylphenyl, Mes*) capped dibenzo[*b*,*f*]borepin (**1b**) and extended "*B*-entacenes" (e.g., **4**) shortly thereafter.[13−15] The *B*-Mes borepins were stable under ambient conditions for a few hours before decomposition,[12] whereas *B*-Mes* borepins were stable indefinitely and could undergo palladium-catalyzed cross-coupling under more chemically aggressive conditions.[16] As π-electron materials, compounds **1**−**4** have drawbacks due to either the lack of long-term ambient stability or bulky Mes* groups that hinder efficient packing necessary for optimal charge transport. Polycyclic aromatic structures with rationally designed heteroatom incorporation are one of the contemporary foundations for cutting-edge organic electronics.[17,18]

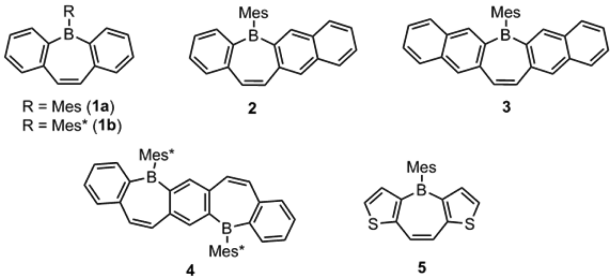

Gronowitz et al. synthesized a dithieno-fused *B*-OH borepin that demonstrated increased stability over the original dibenzo-fused *B*-OH borepin synthesized by van Tamelen.[19,20] These studies in the 1960s on thieno-fused borepins were revisited by Levine et al. in 2014,[9] who synthesized dithieno[*b*,*f*]borepins (e.g., **5**) on gram scales and demonstrated stability under ambient conditions for months with only *B*-Mes substitution. Direct functionalization of the polycyclic borepin was also observed for the first time, and fluoride binding was not inhibited by the mesityl protecting group.[21,22] Analysis of the aromaticity of the borepin ring within the dithieno scaffold by single-crystal X-ray crystallographic and spectroscopic techniques confirms that the π-electron-rich thiophene rings donate electron density into the central borepin ring, comparable to the situation observed in thiophene-fused tropylium-based polycyclic aromatics.[1,19] Terminal fusion of polycyclic aromatics with thiophene rings is a powerful method to alter semi-

Received: April 23, 2016
Published: May 25, 2016

DOI: 10.1021/acs.joc.6b00927
J. Org. Chem. 2016, 81, 5595−5605

Scheme 1. Synthesis of 6

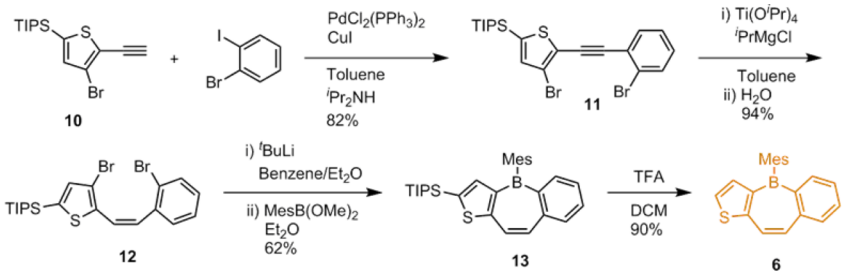

Scheme 2. Synthesis of 7

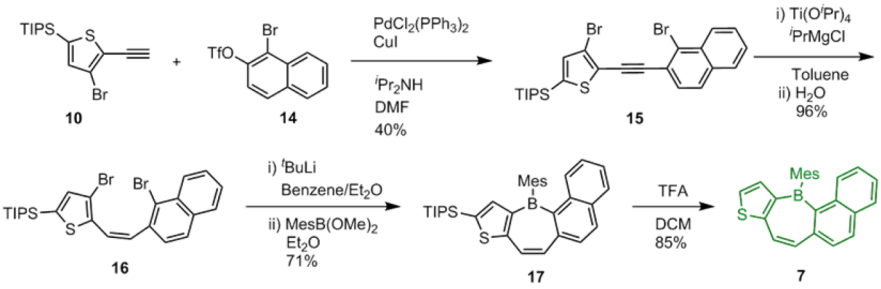

Scheme 3. Synthesis of 8

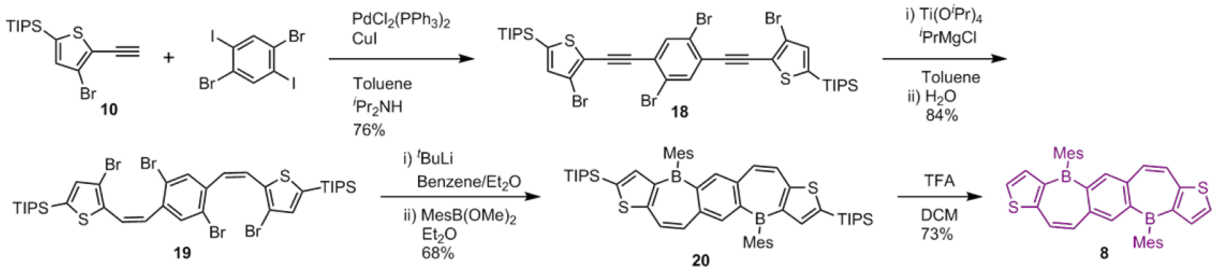

conducting properties. For example, the terminal rings of pentacene have been singly[23] or doubly[24] replaced with thiophene rings to allow for easier chemical functionalization of the extended acene, which can lead to enhanced semiconductor performance.[23,24] Chemical reactivity also varies with these modifications: ring fusion from thiophene to benzo[*b*]thiophene decreases reactivity at the thiophene 2-position while increasing reactivity at the 3-position.[25] Competition for aromaticity can lead to differential localization of electron density within fused ring systems.

In order to evaluate the extent to which competing ring fusions can perturb borepin ring aromaticity, we describe here the synthesis and characterization of new polycyclic borepins that have differential ring fusions. These include examples of benzothieno- (**6**) or naphthothieno- (**7**) flanked borepins along with their larger, C_2-symmetric analogues **8** and **9**, each containing two borepin rings. Additionally, compound **6** can be considered a "hybrid" of C_2-symmetric dibenzoborepin (**1a**) and dithienoborepin (**5**). Both **6** and **7** are also effective model compounds for the larger diborepin-containing species **8** and **9**, respectively. This work demonstrates the borepin ring as an effective reporter of the aromatic competition between fused rings within polycyclic scaffolds. Inspired by Mitchell's studies of *trans*-10b,10c-dimethyldihydropyrene as a ring current reporter of aromaticity in fused ring systems,[26,27] we utilize protons directly attached to the borepin ring as ^{1}H NMR handles to comment on the ring currents in these fused systems.

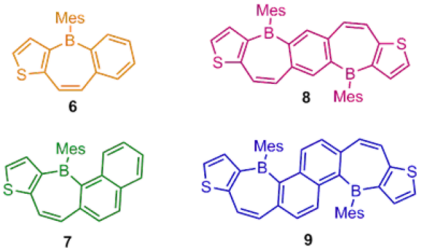

RESULTS AND DISCUSSION

Synthesis. The syntheses of **6**–**9** began with a common precursor (alkyne **10**[28]) and followed similar reactions pathways. The syntheses of **6** and **7** are outlined in Schemes 1 and 2, respectively, and highlight the major synthetic tactics employed in this work. We postulated that diaryl alkynes could be selectively reduced to the *Z*-olefins under Ti-mediated conditions as reported by Moslin et al.[29,30] We previously found that subsequent lithiation of halogens positioned *ortho* to a common *Z*−alkenyl linkage led to direct borepin formation.[9] Thus, we targeted differentially substituted alkynes **11** and **15** as precursors to alkenes **12** and **16**, respectively, after *cis*-selective reduction. Chemoselective Sonogashira coupling with **10** required the use of differentially *ortho*-substituted arenes (1-bromo-2-iodobenzene for **11** and 1-bromonaphthalen-2-yl

DOI: 10.1021/acs.joc.6b00927
J. Org. Chem. 2016, 81, 5595−5605

Scheme 4. Synthesis of 9

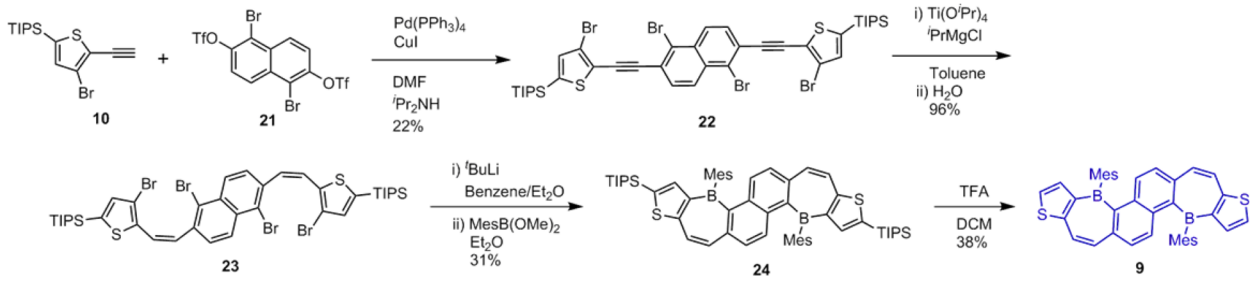

trifluoromethanesulfonate for **14**) where the alkynes coupled at the iodo position in toluene and the triflate position in DMF, respectively. Borepin formation from **12** and **16** was achieved through lithiation and subsequent trapping with $MesB(OMe)_2$, and the TIPS groups were removed after treatment with trifluoroacetic acid (TFA).

Using the same general tactics, we targeted extended structures **8** and **9**. These molecules can be considered as C_2-symmetric versions of the smaller molecules **6** and **7**, joined by a central benzene or naphthalene ring, respectively. The synthesis of compound **8** (Scheme 3) began with chemoselective Sonogashira coupling of 2 equiv of **10** onto 2,5-dibromo-1,4-diiodobenzene, leading to **18**, and the alkynes were reduced under *cis*-selective conditions to form **19**. Direct borepin formation from the alkene gave **20**, and desilylation yielded **8**. The synthesis of **9** (Scheme 4) mirrored the synthesis of **8** with the double coupling of **10** onto **21**, followed by the reduction leading to **23**. The tetrabrominated dialkene **23** was converted to **24** via lithium-halogen exchange and quenching with $MesB(OMe)_2$, and the resulting borepin was desilylated with TFA, thus yielding **9**.

Because of the need to achieve multiple lithiations on one molecular core, the lithiation–borepin formation sequence is usually the most challenging from a reaction design/strategy standpoint. Specifically, solvent selection proved vital for exhaustive tetra-lithium-halogen exchanges without unwanted side reactions.[31,32] A series of Li-Br exchanges (Figure S-52) revealed a hexane:Et_2O solvent mixture (95:5) to be optimal for direct borepin formation. Under these conditions, the 4-fold lithium-halogen exchange, followed by quenching with dimethoxymesitylborane, led to the targeted borepin compounds in good yields (30–70%). The triisopropylsilyl groups were required for successful borepin conversion from the respective *Z*-alkene: reactions on desilylated substrates were complicated by the acidic α-protons on the thiophene rings, which may have promoted "halogen dance" related complexities.[33] Intriguingly, the triisopropylsilyl groups could not be removed after treatment with tetrabutylammonium fluoride and required trifluoroacetic acid, which had been noted previously with a triisopropylsilyl protected pentathienoacene.[34]

Characterization. Aromaticity is a multidimensional series of characteristics[35,36] most commonly defined by energetic,[37,38] local-geometric[39] and magnetic[26,40] terms, as is manifested by chemical reactivity, molecular planarity, and electronic considerations.[41] Defining and quantifying aromaticity in an absolute sense remains an elusive goal, but a combination of theoretical, computational, and experimental work continues to develop unifying concepts.[42] The electronic properties of **6**–**9** were analyzed by UV–vis and PL spectroscopy, and the electrochemical properties were determined by CV in order to understand gross electronic delocalization within the polycyclic molecules.[43] Single-crystal X-ray crystallography was employed to shed light on the structural influence of various ring fusions while ^1H NMR spectroscopy was used to further inform on the aromatic character. DFT calculations including optimized gas-phase geometries, molecular orbital contour plots, and gauge-independent atomic orbital (GIAO) calculations were carried out on **1**–**9**.

UV–vis and Photoluminescence. Figure 1 displays the UV–vis spectra of **6** and **8** (Figure 1a) and **7** and **9** (Figure 1b).

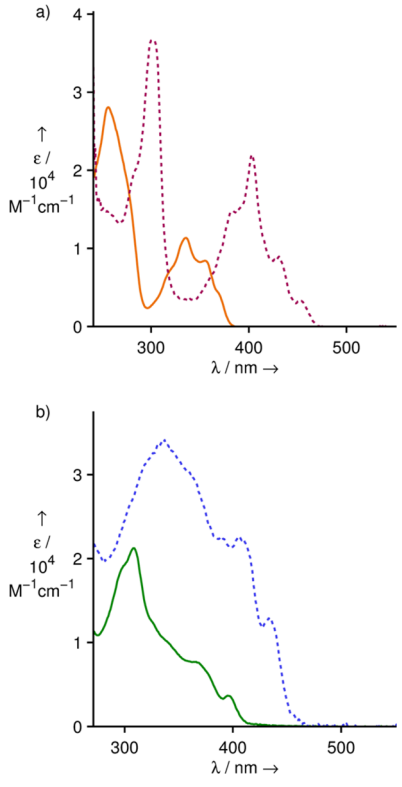

Figure 1. UV–vis spectra in $CHCl_3$ of (a) **6** (orange solid), **8** (red dotted) and (b) **7** (green solid), **9** (blue dotted).

Benzene-fused **6** and **8** display similar absorption signatures with a high energy feature (256 nm for **6**; 302 nm for **8**) and lower energy series of vibronic transitions (310–350 nm for **6**; 380–420 nm for **8**), with onsets at 390 nm for **6** and 460 nm for **8**. Both naphthalene-fused compounds display broad and ill-defined features with absorptions onsets at 416 nm for **7** and 473 nm for **9**. The extended structures **8** and **9** have bathochromic shifts relative to their respective model compounds due to the extension of carbon-centered π-conjugation through the 1,4-positions of the benzene of **8** and the 2,6-positions of the naphthalene of **9**.[44] These

DOI: 10.1021/acs.joc.6b00927
J. Org. Chem. 2016, 81, 5595–5605

absorbance trends are consistent with trends found in other molecules including **1a** (262 nm), **2** (280 nm), and **3** (314 nm) where the absorption maxima increase with acene extension (Table 1). Molecules **7** and **9** cannot be compared to naphthalene fused borepins **2** and **3** because of the different isomeric fusion relationships between borepin and naphthalene rings. Storage of **8** in the solid state was shown to have minimal degradation over 6 months, but significant changes were found in the UV−vis spectrum of a solution of **8** stored over the same time period (Figure S-54). These results suggest that a single thiophene fusion on the borepin ring is enough to impart long-term ambient stability in the solid state with *B*-Mes protecting groups.

Table 1. Photophysical and Electrochemical Properties of Selected Compounds

	λ_{abs}/nm	λ_{em}/nm	QY/%[a]	$E_{1/2}$/V[b]
1a[12]	262	400	70	−2.56
2[12]	280	445	39	−2.25
3[12]	314	477	1	−2.20
4[14]	286	456	71	−2.10
5[9]	266	392	6	−2.46
6	256	384	6	−2.51
7	308	431	6	−2.27
8	302	469	8	−2.09
9	337	452	19	−2.14

[a]Relative to quinine sulfate (0.55). [b]All potentials are referenced to the Fc/Fc^+ redox couple.

The exchange of benzene fusions for naphthalene fusions on the central borepin ring (**1a**, **2**, and **3**) decreases the quantum yields and shifts the λ_{max} to lower energies in a manner consistent with increasing conjugation.[12] From 3 to 4 to 5 rings in these new polycyclic cores, the λ_{max} increases as would be expected (**6**: 384 nm; **7**: 431 nm; **8**: 469 nm); however, for **9** (452 nm) where there are 6 fused rings, the λ_{max} maximum is less than **8** (Figure 2). Similar electronic trends have been observed for linear vs angular polyacenes and have been rationalized by increased aromatic character in the zigzag systems.[45,46]

Electrochemistry. The CVs of **6**−**9** were compared to model literature compounds (Table 1) and are shown in Figures S38−S43. Increasing conjugation typically decreases the formal reduction potential ($E_{1/2}$), and this trend was conserved across multiple series of borepin-containing molecules. Dibenzoborepin (**1a**) had a reduction potential of −2.56 V while benzothienoborepin (**6**) was more easily reduced at −2.51 V and dithienoborepin (**5**) was even more easily reduced at −2.46 V. This is consistent with previous reports where thiophene-fused acenes have lower LUMO levels and are more easily reduced than all-carbon equivalents.[23] Despite the increase in the number of rings, compound **8** (−2.09 V) is more easily reduced than **9** (−2.14 V), which suggests a more stable zigzag system.[46]

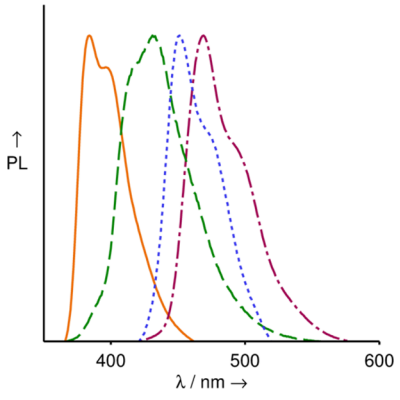

Figure 2. Normalized photoluminescence spectra of **6** (orange solid) and **7** (green dashed) excited at 350 nm; **8** (red dashed-dotted) and **9** (blue dotted) excited at 400 nm in $CHCl_3$.

Single-Crystal X-ray Crystallography. The packing motifs obtained from the crystal structures are shown in Figure 3 and are viewed edge-on along the long axis to clearly display key interactions between individual molecules. The edge-to-face packing of **6** (Figure 3a) transitions to offset edge-to-face in the diborepin analogue **8** (Figure 3c) both with ca. 3.6 Å distances between the center of the borepin ring and the base of the borepin ring from a neighboring molecule in a herringbone fashion.[47] The tricyclic core of **6** is slightly bowed with deviation from the borepin plane of 8.9° to the thiophene plane and 8.8° to the benzene plane. The pentacyclic core of **8** is more planar with deviations between the borepin−thiophene planes of 6.2° and borepin−benzene planes of 5.4°. Interactions between **7** (Figure 3b) and **9** (Figure 3d) are dominated by methyl groups on mesityl rings with naphthyl or thienyl groups on adjacent molecules with distances of ca. 3.4 Å. The kinetic blocking groups necessary to protect boron from adventitious nucleophiles drive apart the acene cores of **7** to ca. 5−6 Å. The four-ring core of **7** is significantly twisted, with deviations of 6.3° between the borepin−thiophene planes, 12.4° between borepin−naphthalene planes, and even a deviation from planarity between two rings of the naphthalene core of 6.4°. The six ring core of **9** is more planar with the overall smallest thiophene−borepin plane deviation of 4.1°, a large borepin−naphthalene plane deviation of 14.7°, but with a planar naphthalene unit.

Bond length alternation (or lack thereof) is one of the oldest metrics to quantify structural aromaticity, and it can be observed experimentally and investigated computationally.[39,48] The circulation of electrons associated with aromaticity engenders observable magnetic properties (e.g., deshielding of ring protons), which can be correlated with calculated NMR shielding tensors. Heteroatom involvement further complicates the experimental assessment of aromaticity, thus adding value to nucleus-independent chemical shift (NICS) values.[49,50] Despite recent debates about the viability of NICS calculations for predicting aromaticity, especially in polycyclic fused aromatics,[40,51] NICS calculations are reasonable for confirming the local magnetic properties of some fused ring systems.[52,53]

The structural criteria for aromaticity can be experimentally observed in the degree of bond length alternation. The selected bond lengths in Table 2 lend themselves well to this task as the shortest B−C_α and C_γ−C_γ bonds (Figure 4) in **1**−**9** are not directly obscured by any ring fusions and, therefore, report on the local borepin scaffold. The B−C_α bond is the longest bond in the borepin ring due to the radius of the boron atom, and it should contract with increased aromatic character. Conversely, the olefinic C_γ−C_γ bond is an excellent handle because it is also decoupled from any ring fusions and should increase in length with aromatic character from that of a localized alkene (ca. 1.34 Å) to that of a delocalized benzene (ca. 1.40 Å).[1] While the σ framework of an aromatic system has been implicated in bond

DOI: 10.1021/acs.joc.6b00927
J. Org. Chem. 2016, 81, 5595−5605

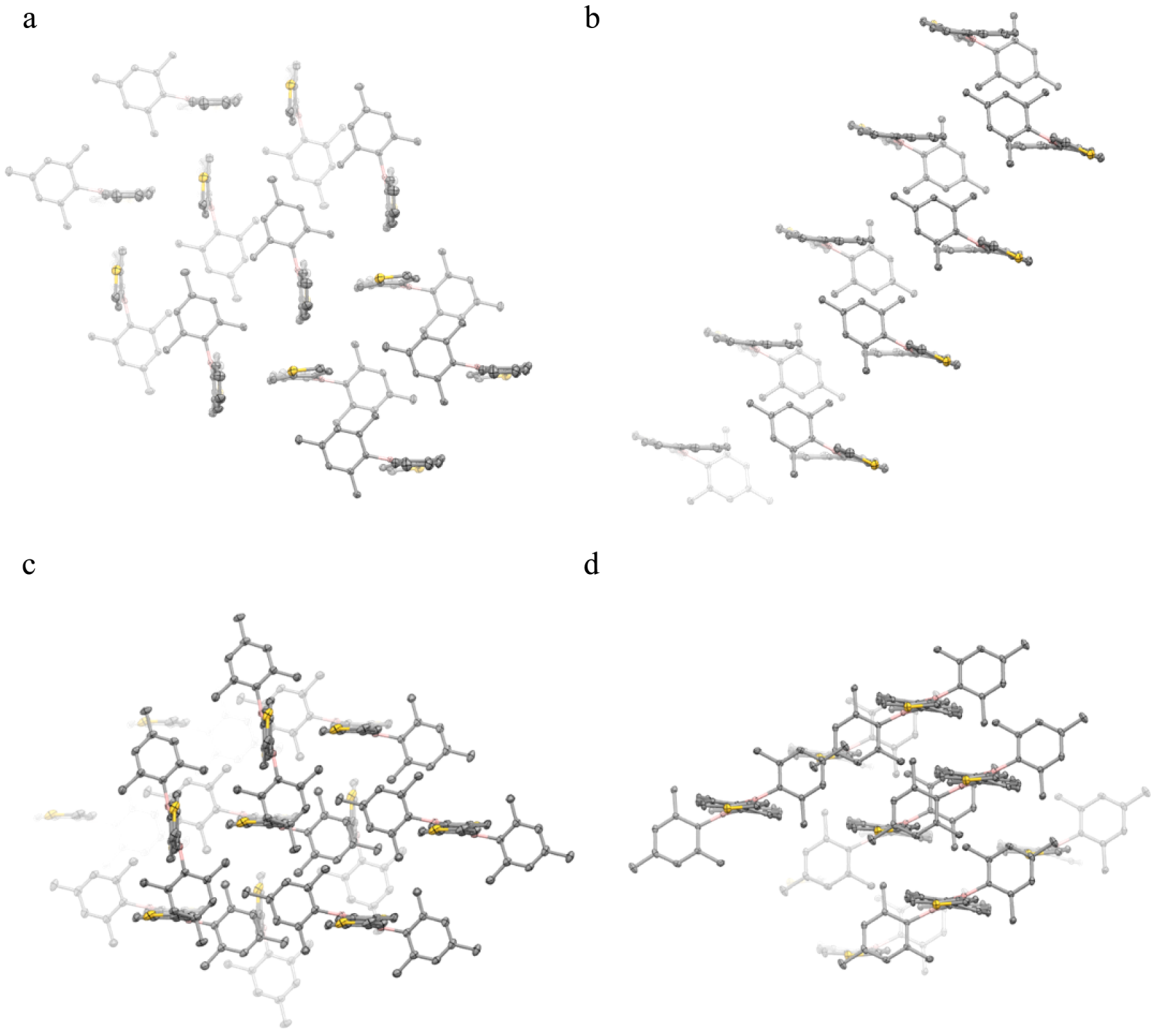

Figure 3. Displacement ellipsoid plots (50% probability level) at 110(2) K showing crystal packing along the plane of the borepin ring(s) of (a) **6**, (b) **7**, (c) **8**, and (d) **9**.

Table 2. Selected Bond Lengths and ^{1}H NMR Resonances (in $CDCl_3$)

	B–$C_{\alpha\text{-t}}$/Å	B–$C_{\alpha\text{-c}}$/Å	C_γ–C_γ/Å	$^1H_{\gamma\text{-t}}$/ppm	$^1H_{\gamma\text{-c}}$/ppm
1a[57]		1.564(3)	1.342(3)		7.37
		1.563(2)			
2[12]		1.561(3)	1.346(3)		7.41
		1.568(3)			7.20
3[12]		1.559(3)	1.338(3)		7.27
		1.566(3)			
4[14]		1.570(3)	1.341(3)		
		1.573(3)			
5[9]	1.533(2)		1.348(2)	7.69	
	1.538(2)				
6	1.542(5)	1.545(4)	1.371(5)	7.66[a]	7.41[a]
7	1.546(2)	1.563(2)	1.348(2)	7.77[a]	7.57[a]
8	1.536(2)	1.559(2)	1.352(2)	7.55[a]	7.41[a]
9	1.550(2)	1.566(2)	1.349(2)	7.74[a]	7.44[a]

[a]Tentative assignment based on calculated values.

length equalization, the π-framework is often viewed as dictating the extent of delocalization.[44,54−56] The experimentally determined bond lengths obtained from crystal structures are, therefore, critical tools for evaluating aromaticity.

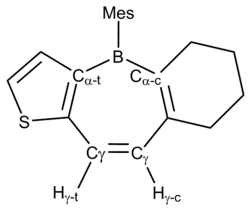

Figure 4. A generic borepin showing key carbon atoms associated with thieno ($C_{\alpha\text{-t}}$) and carbocyclic ($C_{\alpha\text{-c}}$) ring fusions, and key ring protons rendered chemically inequivalent by the different thieno ($H_{\gamma\text{-t}}$) and carbocycle ($H_{\gamma\text{-c}}$) ring fusions. These protons are attached to the unfused carbons (C_γ) on the borepin skeleton.

Intraring B–C bond lengths are found to be shorter than exocyclic *B*–Mes bonds, and this contraction indicates delocalization around the borepin ring.[8] The B–C_α bonds contract in tricyclic molecules from **1a** to **6** to **5**, suggesting an increasing degree of borepin-centered aromaticity (Table 2). The B–$C_{\alpha\text{-c}}$ bonds in **1a** (1.564(3) and 1.563(2) Å) were equal within experimental error; however, there was a twist in the tricyclic core of **5**, leading to two unique B–$C_{\alpha\text{-t}}$ bond lengths (1.533(2) and 1.538(2) Å). The B–C_α bonds in **6** (B–$C_{\alpha\text{-t}}$: 1.542(5) Å and B–$C_{\alpha\text{-c}}$: 1.545(4) Å) have intermediate length between the C_2-symmetric comparison compounds; however,

DOI: 10.1021/acs.joc.6b00927
J. Org. Chem. 2016, 81, 5595−5605

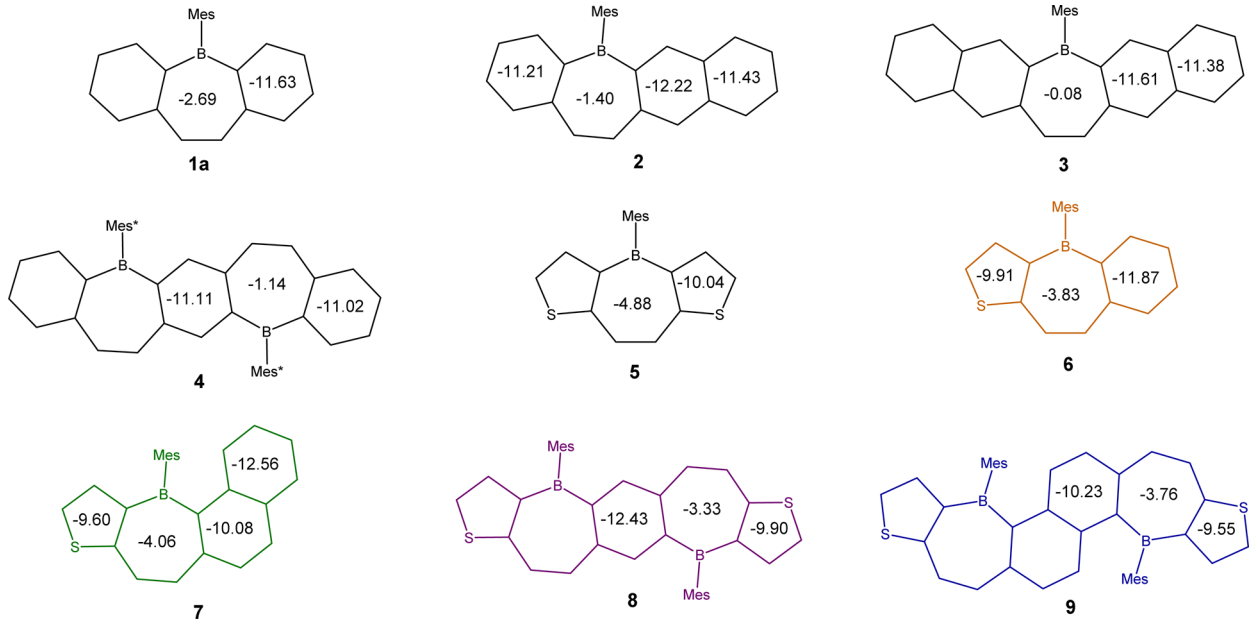

Figure 5. Isotropic NICS(1) calculations 1 Å above the center of each ring (in ppm).

the C_γ−C_γ bonds remain mostly unchanged from **1a** to **6** to **5**. The pentacyclic compounds **4** and **8** further demonstrate the influence of competing arene and thiophene ring fusions in a *para*-phenylene diborane fashion. The B−C_α bonds of **8** (B−$C_{\alpha\text{-t}}$: 1.536(2) Å and B−$C_{\alpha\text{-c}}$: 1.559(2) Å) are shorter, and the C_γ−C_γ bond of **8** (1.352(2) Å) is longer than the respective bonds in **4** (B−$C_{\alpha\text{-c}}$: 1.570(3) and 1.573(3) Å; C_γ−C_γ: 1.341(3) Å). This indicates increased aromatic character in the borepin rings of **8** relative to **4** due to the weaker aromaticity of the competiting thiophene fusion and allows for the borepin ring to vie for additional aromatic character. The trend continues with **5**, which has two thiophene rings fused on either side of the borepin ring that can donate additional aromaticity, and it has an even longer C_γ−C_γ bond and shorter B−C_α bonds.

As additional points of comparison, molecule **8** has a more olefinic C_γ−C_γ bond than **6**, which suggests less local aromatic character in the borepin ring of **8** relative to **6**. We attribute this to the *para*-phenylene diborane unit in **8** that diminishes the relative influence of the benzene center. The corresponding contraction of B−C_α is not observed from **6** to **8** likely due to packing effects as the mesityl group of **6** is distorted out of the acene plane. Compounds **7** and **9** cannot be directly compared with the other naphtho-fused borepins (**2** and **3**) because of the internal steric clashing of the mesityl ring with the naphthalene ring protons. This leads to a twisting of the mesityl ring and naphthalene ring away from each other to reduce repulsive forces. The B−C_α bond contraction of **7** relative to **9** is observed; however, the C_γ−C_γ bonds are equal within experimental error.

Nuclear Magnetic Resonance. The magnetic properties of aromatic compounds can be measured experimentally utilizing ^{1}H NMR spectroscopy.[40] The ^{1}H resonances of the olefinic protons (H_γ) directly attached to the borepin ring (Figure 4) are effective handles for evaluating local ring currents. They are geometrically distanced from any heteroatoms and are available in all of the comparison compounds. Contributions from local heteroaromaticity and the diamagnetic anisotropy from neighboring rings could influence these resonances, but the greatest influences should be expected from the borepin ring aromaticity. The ^{1}H NMR spectra of borepin precursors **12**, **16**, **19**, and **23** revealed two olefinic doublets at ca. 6.5 ppm with coupling constants of ca. 12 Hz. After borepin formation, the two doublets still with ca. 12 Hz coupling were centered closer to ca. 7.5 ppm. These resonances are easily identifiable when compared with thienyl, benzyl, or naphthyl protons due to their respective coupling constants. However, the proximity to other aromatic resonances prevented definitive NOESY or COSY assignment of the $^1H_{\gamma\text{-t}}$ and $^1H_{\gamma\text{-c}}$ resonances (shown in Figure 4). DFT calculations (GIAO, B3LYP/G-31(d,p)) predicted isotropic NMR shielding tensors that matched up well with experimentally observed resonances (Figure S-53), and these data were used to make tentative assignments. The H_γ protons attached to borepins with more local aromaticity were slightly deshielded progressing from **1a** ($^1H_{\gamma\text{-c}}$: 7.37 ppm) to **6** ($^1H_{\gamma\text{-c}}$: 7.41 ppm and $^1H_{\gamma\text{-t}}$: 7.66 ppm) to **5** ($^1H_{\gamma\text{-t}}$: 7.69 ppm). The H_γ protons of **6** are more deshielded than **8** ($^1H_{\gamma\text{-c}}$: 7.41 ppm and $^1H_{\gamma\text{-t}}$: 7.55 ppm), indicating increased diamagnetic anisotropy, which agrees with the crystallographic assessment. Compound **7** ($^1H_{\gamma\text{-c}}$: 7.57 ppm and $^1H_{\gamma\text{-t}}$: 7.77 ppm) has more deshielded H_γ protons than **9** ($^1H_{\gamma\text{-c}}$: 7.44 ppm and $^1H_{\gamma\text{-t}}$: 7.74 ppm), also revealing increased aromatic character in the borepin ring of **7** compared with **9**.

This experimental evidence of differential electron circulation/aromaticity was corroborated by NICS(1) calculations. NICS(1) values were calculated 1 Å above the center of each unique ring of **1**−**9** using DFT (B3LYP/6-31G(d,p)), and the results are displayed in Figure 5. The NICS(1) values for the borepin rings of **1** (−2.69), **2** (−1.40), and **3** (−0.08) corroborate the increased shielding values of the respective H_γ protons and indicate a decrease in ring current around the borepin ring as fusion changes from benzene to naphthalene. The exchange of benzene for thiophene fusion that led to deshielding of the H_γ protons is correctly predicted by a decrease in the NICS(1) value moving from **1a** (−2.69) to **6** (−3.83) to **5** (−4.88). The single borepin-containing molecules **6** (−3.83) and **7** (−4.06) have more negative NICS(1) values compared with diborepin species **8** (−3.33) and **9** (−3.76). For

DOI: 10.1021/acs.joc.6b00927
J. Org. Chem. 2016, 81, 5595−5605

both cases, the naphthalene fusion enables more aromatic ring current within the borepin moiety versus benzene. Although the two distinct $^1H_\gamma$ resonances of **4** could not be explicitly assigned, the borepin ring NICS(1) value of **4** (−1.14) is less negative than **8** (−3.33), which indicates increased ring current in thieno-fused borepins and is consistent with the trend between **1a** and **5**. These calculations further corroborate the experimental findings showing how differential aromatic fusions can attenuate the local borepin aromaticities in fused molecules.

■ CONCLUSIONS

New borepin molecules with differential carbocyclic and thieno ring fusions were characterized and compared to model molecules. Local borepin aromaticity was generally found to increase with the exchange of strongly aromatic benzene fusions for the electron-rich, less aromatic thiophene ring fusions as determined by geometric, magnetic, and computational assessments. The borepin ring of the "hybrid" thieno-benzoborepin **6** expressed intermediate levels of aromatic character between corresponding dibenzoborepin **1** and dithienoborepin **5**. Both diborepin-containing species **8** and **9** showed less local borepin aromatic character than their respective model compounds **6** and **7**. Overall, these compounds are the first examples of differentially fused [*b*,*f*]borepins and displayed aromatic properties that bridge the gap between arene and thiophene-fused borepins. Even with one thiophene fusion, the chemical stability due to the electron-rich thiophene unit demonstrates the ability to work with structures that previously required bulkier protecting groups or exhibited reduced long-term stability.

■ EXPERIMENTAL SECTION

All reactions were carried out under an atmosphere of purified nitrogen using Schlenk techniques unless noted otherwise. All solvents were degassed by sparging with nitrogen and were then stored over molecular sieves to remove trace amounts of water. All reagents were analytical grade and used without further purification unless otherwise noted. Dimethoxymesitylborane,[58] 1-bromonaphthalene-2-ol, 1,5-dibromonaphthalene-2,6-diol,[59] and **10**[28] were synthesized according to literature procedures. 2,5-Dibromo-1,4-diiodobenzene, 1-bromo-2-iodobenzene, 2-hydroxynaphthalene, and 2,6-dihydroxynaphthalene were purchased and used without further purification. All ^{13}C and ^1H NMR spectra were recorded on a 400 MHz instrument and were taken in either deuterated chloroform (the signal for residual protio solvent was set at 7.26 ppm for ^1H NMR, and the carbon signal was also set on the solvent peak at 77.16 ppm for ^{13}C NMR) or deuterated dichloromethane (the signal for residual protio solvent was set at 5.32 ppm for ^1H NMR, and the carbon signal was also set on the solvent peak at 53.84 ppm for ^{13}C NMR). High-resolution mass spectra (HRMS) were obtained with electron impact (EI) or fast-atom bombardment (FAB) ionization and analyzed by double focusing magnetic sectors. Solutions of *n*-butyllithium and *t*-butyllithium were titrated with diphenylacetic acid, and *i*-propylmagnesium chloride was titrated with salicylaldehyde hydrazine before use.

Photophysical Considerations. Spectroscopic measurements were conducted in $CHCl_3$ solutions at room temperature on a UV−vis spectrometer. Photoluminescence spectra were recorded on a fluorometer with a 75 W xenon lamp while maintaining solution optical densities below 0.1 au. Quantum yields were determined relative to quinine sulfate in 0.05 M H_2SO_4 (55%).

Electrochemical Considerations. Cyclic voltammetry was performed in a one-chamber, three-electrode cell using a potentiostat. A 2 mm^2 Pt button electrode was used as the working electrode with a platinum wire counter electrode relative to a quasi-internal Ag wire reference electrode submersed in 0.01 M $AgNO_3$/0.1 M *n*-Bu_4NPF_6 in anhydrous acetonitrile. Measurements were taken on millimolar analyte concentrations in 0.1 M *n*-Bu_4PF_6 (in THF) electrolyte solutions recorded at a scan rate of 100 mV/s. Potentials were recorded relative to the Ag/Ag^+ couple and are reported relative to the Fc/Fc^+ (Table 1) couple ca. + 23 mV vs our Ag/Ag^+ reference.

Computational Considerations. Molecular orbital calculations were performed at the DFT level (B3LYP/6-31G(d,p)) on equilibrium geometries using Gaussian 09.[60]

*(4-Bromo-5-((2-bromophenyl)ethynyl)thiophen-2-yl)triisopropylsilane (**11**).* $PdCl_2(PPh_3)_2$ (208 mg, 0.296 mmol) and CuI (113 mg, 0.593 mmol) were added to a dry, nitrogen-filled 500 mL Schlenk flask. Toluene (200 mL), diisopropylamine (50 mL), and 2-bromo-1-iodobenzene (1.25 mL, 9.73 mmol) were added to the flask, and the solution was stirred at room temperature. In a dry, nitrogen-filled 25 mL round-bottom flask, **10** (3.36 g, 9.79 mmol) was dissolved in diisopropylamine (20 mL). A cannula was used to transfer the alkyne solution into the reaction flask over 30 min, and the mixture was stirred at room temperature for 20 h, at which point it was poured through a pad of Celite and eluted with hexane. A 5% NH_4Cl solution was added and extracted against hexane (3×). The combined organic layers were washed with brine, dried over anhydrous $MgSO_4$, and concentrated under reduced pressure to provide a brown solid that was further purified by column chromatography (SiO_2:hexane) to yield **11** as a yellow solid (3.97 g, 7.97 mmol, 82%) with trace alkyl impurities. ^1H NMR (400 MHz, $CDCl_3$) δ: 7.62 (ddd, 1H, J = 0.4, 1.2, 8.0 Hz), 7.57 (ddd, 1H, J = 0.4, 1.7, 7.7 Hz), 7.30 (dt, 1H, J = 1.2, 7.6 Hz), 7.20 (td, 1H, J = 1.7, 7.8 Hz), 7.11 (s, 1H), 1.31 (sept, 3H, J = 7.2 Hz), 1.11 (d, 18H, 7.3 Hz). ^{13}C {^1H} NMR (100 MHz, $CDCl_3$) δ: 139.2, 137.8, 133.4, 132.7, 129.9, 127.2, 125.39, 125.23, 125.2, 117.6, 96.4, 85.7, 18.6, 11.8. HRMS (EI) found m/z = 495.9903 (M^+), calculated for $C_{21}H_{26}Br_2SSi$: 495.9891.

*(Z)-(4-Bromo-5-(2-bromostyryl)thiophen-2-yl)triisopropylsilane (**12**).* A solution of **11** (90.0 g, 0.181 mmol), titanium isopropoxide (0.23 mL, 0.78 mmol) in toluene (20 mL) was set to stir in a 100 mL Schlenk tube. A solution of *i*-propylmagnesium chloride in Et_2O (2.00 M, 0.90 mL, 1.8 mmol) was added in a single portion, and the reaction was stirred for 10 min at −78 °C in an acetone and dry ice bath and then warmed to −40 °C in an acetonitrile and dry ice bath for 3 h. Water (1 mL) was added to the cooled solution, which was then allowed to slowly warm to room temperature over 17 h. The reaction mixture was diluted with 1 M HCl and extracted with hexane (3×), and the combined organic layers were washed with brine, dried over anhydrous $MgSO_4$, filtered, and concentrated under reduced pressure. The crude solid was further purified by a short chromatographic plug (SiO_2:hexane) to yield **12** as a yellow solid (84.9 mg, 0.710 mmol, 94%) with trace alkyl impurities. ^1H NMR (400 MHz, $CDCl_3$) δ: 7.62 (dd, 1H, J = 1.5, 7.7 Hz), 7.35 (dd, 1H, J = 2.0, 7.0 Hz), 7.18 (m, 2H), 7.00 (s, 1H), 6.85 (d, 1H, J = 12 Hz), 6.65 (d, 1H, J = 12 Hz), 1.15 (sept, 3H, J = 7.0 Hz), 1.00 (d, 18H, J = 7.2 Hz). ^{13}C {^1H} NMR (100 MHz, $CDCl_3$) δ: 138.4, 137.4, 137.0, 135.9, 132.9, 131.4, 130.1, 129.6, 127.3, 124.0, 123.0, 113.9, 18.6, 11.6. HRMS (EI) found m/z = 498.0031 (M^+), calculated for $C_{21}H_{28}Br_2SSi$: 498.0048.

*2-Triisopropylsilyl-4-mesitylbenzo[1′,2′:6,7]borepino[3,2-b]thiophene (**13**).* A solution of **12** (54.8 mg, 0.110 mmol), benzene (12 mL), and Et_2O (0.4 mL) was cooled to 5 °C in an ice and water bath. A solution of *t*-butyllithium in hexanes (1.61 M, 0.27 mL, 0.44 mmol) was added dropwise, and the solution was stirred for 2 min. A solution of $MesB(OMe)_2$ in Et_2O (0.31 M, 0.38 mL, 0.12 mmol) was added dropwise by syringe to the reaction vessel. The reaction mixture was allowed to slowly warm to room temperature over 19 h. The reaction mixture was diluted with 5% NH_4Cl, and the aqueous layer was extracted with hexane (3×). The combined organic layers were washed with brine, dried over anhydrous $MgSO_4$, filtered, and concentrated under reduced pressure. The crude solid was further purified by column chromatography (SiO_2:hexane) to yield **13** as a yellow solid (32.1 mg, 0.0682 mmol, 62%) with trace alkyl impurities. ^1H NMR (400 MHz, $CDCl_3$) δ: 8.12 (dd, 1H, J = 1.5, 7.8 Hz), 7.90 (dt, 1H, J = 0.6 Hz, 7.9 Hz), 7.74 (m, 1H), 7.66 (dd, 1H, J = 0.6, 12 Hz), 7.46 (m, 1H), 7.41 (d, 1H, J = 12 Hz), 6.90 (d, 2H, J = 0.6 Hz), 2.40 (s, 3H), 1.91 (s, 6H), 1.27 (sept, 3H, J = 7.4 Hz), 1.05 (d, 18H, J = 7.3 Hz). ^{13}C {^1H} NMR (100 MHz, $CDCl_3$) δ: 160.9, 148.2, 144.3, 141.3,

DOI: 10.1021/acs.joc.6b00927
J. Org. Chem. 2016, 81, 5595−5605

137.9, 136.1, 135.9, 134.3, 132.6, 132.1, 127.5, 127.0, 123.7. HRMS (EI) found m/z = 470.2643 (M^+), calculated for $C_{30}H_{39}BSSi$: 470.2635.

*4-Mesitylbenzo[1′,2′:6,7]borepino[3,2-b]thiophene (**6**).* Trifluoroacetic acid (0.9 mL) was added in 3 portions over 3 h to a solution of **13** (56.3 mg, 0.120 mmol) in CH_2Cl_2 (25 mL) under a N_2 atmosphere. The solution was stirred in the absence of light, and the reaction progress was monitored by TLC. The reaction mixture was diluted with water and extracted with $CHCl_3$ (3×). The combined organic layers were washed with brine, dried over anhydrous $MgSO_4$, filtered, and concentrated under reduced pressure. The crude solid was further purified by column chromatography (SiO_2:hexane) to yield **6** as a pure white solid (33.8 mg, 0.108 mmol, 90%). ^{1}H NMR (400 MHz, CD_2Cl_2) δ: 8.09 (dd, 1H J = 1.5, 7.8 Hz), 7.95 (dt, 1H, J = 0.6, 7.9 Hz), 7.78 (td, 1H, J = 1.6, 7.1 Hz), 7.65 (d, 1H, J = 12 Hz), 7.49 (m, 2H), 7.42 (d, 1H, J = 5.2 Hz), 7.22 (dd, 1H, J = 0.7, 5.2 Hz), 6.93 (d, 2H, J = 0.6 Hz), 2.39 (s, 3H), 1.89 (s, 6H). ^{13}C {^{1}H} NMR (100 MHz, CD_2Cl_2) δ: 157.1, 144.6, 141.4, 138.9, 138.0, 136.7, 134.6, 133.4, 132.6, 128.0, 127.4, 126.3, 124.3, 22.9, 21.4. HRMS (EI) found m/z = 314.1303 (M^+), calculated for $C_{21}H_{19}BS$: 314.1301.

*1-Bromonaphthalen-2-yl Trifluoromethanesulfonate (**14**).* A 25 mL Schlenk flask was charged with 1-bromonaphthalene-2-ol (1.75 g, 7.85 mmol), DCM (80 mL), and a stir bar under N_2. Pyridine (12 mL) was added, and the solution was cooled to 0 °C in an ice and water bath. Trifluoromethanesulfonic anhydride (3.00 mL, 17.8 mmol) was added dropwise, and the mixture was allowed to stir for 18 h and warm up to room temperature. The reaction mixture was diluted with 1 M HCl and extracted with $CHCl_3$ (3×). The combined organic layers were dried with $MgSO_4$, filtered, and removed under reduced pressure to provide a brown solid that was further purified by a short chromatographic plug (SiO_2: 80% hexane, 20% EtOAc) to yield **14** as a pure white solid (2.62 g, 7.37 mmol, 94%). ^{1}H NMR (400 MHz, CD_2Cl_2) δ: 8.34 (m, 1H), 7.95 (m, 2H), 7.73 (m, 1H), 7.66 (m, 1H), 7.46 (d, 1H, J = 9.0 Hz). ^{13}C {^{1}H} NMR (100 MHz, CD_2Cl_2) δ: 145.5, 133.4, 133.0, 130.3, 129.2, 128.8, 128.2, 127.9, 120.2, 120.1, 116.5. HRMS (EI) found m/z = 353.9175 (M^+), calculated for $C_{11}H_6BrF_3O_3S$: 353.9173.

*(4-Bromo-5-((1-bromonaphthalen-2-yl)ethynyl)thiophen-2-yl)-triisopropylsilane (**15**).* A 100 mL Schlenk flask was charged with $PdCl_2(PPh_3)_2$ (218 mg, 0.310 mmol), CuI (116 mg, 0.609 mmol), **14** (2.24 g, 6.29 mmol), and stir bar. Dimethylformamide (150 mL) and diisopropylamine (50 mL) were added, and the mixture was allowed to stir at room temperature. A solution of **10** (2.12 g, 6.17 mmol) in diisopropylamine (30 mL) was transferred by cannula to the reaction mixture over 30 min, and the mixture was stirred for 20 h. The reaction was diluted with a 1 M HCl solution, and the aqueous layer was extracted against hexane (5×). The combined organic layers were washed with a saturated solution of 5% NH_4Cl and washed with brine, anhydrous $MgSO_4$, and filtered, and the solvent was removed under reduced pressure. The crude product was further purified with a chromatographic column (SiO_2:hexane) to afford the desired product as a yellow solid **15** that was used without further purification (1.46 g, 2.50 mmol, 40%). ^{1}H NMR (400 MHz, $CDCl_3$) δ: 8.32 (d, 1H, J = 8.5 Hz), 7.81 (d, 1H, J = 8.0 Hz), 7.77 (d, 1H, J = 8.3 Hz), 7.58 (m, 3H), 7.14 (s, 1H), 1.33 (sept, 3H, J = 7.1 Hz), 1.13 (d, 18H, 7.3 Hz). ^{13}C {^{1}H} NMR (100 MHz, $CDCl_3$) δ: 139.3, 137.8, 133.9, 132.4, 128.9, 128.4, 128.1, 128.0, 127.7, 127.5, 126.4, 125.4, 123.2, 117.7, 97.8, 86.5, 18.6, 11.8. HRMS (EI) found m/z = 546.0032 (M^+), calculated for $C_{25}H_{28}Br_2SSi$: 546.0048.

*(Z)-(4-Bromo-5-(2-(1-bromonaphthalen-2-yl)vinyl)thiophen-2-yl)triisopropylsilane (**16**).* A solution of **15** (1.18 g, 2.16 mmol), titanium isopropoxide (1.7 mL, 5.7 mmol) in toluene (200 mL) was set to stir in a 500 mL Schlenk tube. A solution of *i*-propylmagnesium chloride in Et_2O (1.61 M, 8.0 mL, 13 mmol) was added in a single portion, and the reaction was stirred for 30 min at −78 °C in an acetone and dry ice bath and then warmed to −40 °C in an acetonitrile and dry ice bath for 2 h. Water (10 mL) was added to the cooled solution, which was then allowed to warm to room temperature over 18 h. The reaction mixture was diluted with 1 M HCl and hexane, and the aqueous layer was extracted against hexane (3×). The combined organic layers were washed with brine, dried over anhydrous $MgSO_4$, filtered, and concentrated under reduced pressure. The crude solid was further purified by a short chromatographic plug (SiO_2:hexane) to yield **16** as a yellow solid (2.08 g, 1.14 mmol, 96%) with trace alkyl impurities. ^{1}H NMR (400 MHz, $CDCl_3$) δ: 8.35 (d, 1H, J = 7.8 Hz), 7.80 (d, 1H, J = 8.0 Hz), 7.67 (d, 1H, J = 8.4 Hz), 7.59 (m, 1H), 7.53 (m, 1H), 7.41 (d, 1H, J = 8.5 Hz), 6.92 (d, 1H, J = 12 Hz), 6.88 (d, 1H, J = 12 Hz), 1.08 (sept, 3H, J = 7.2 Hz), 0.92 (d, 18, J = 7.2 Hz). ^{13}C {^{1}H} NMR (100 MHz, $CDCl_3$) δ: 138.5, 137.0, 136.1, 135.6, 134.3, 132.8, 131.1, 128.3, 128.2, 127.5, 127.4, 126.8, 124.4, 122.9, 113.8, 105.1, 18.5, 11.5. HRMS (EI) found m/z = 548.0188 (M^+), calculated for $C_{25}H_{30}Br_2SSi$: 548.0204.

*10-Triisopropylsilyl-12-mesitylnaphtho[2′,1′:6,7]borepino[3,2-b]-thiophene (**17**).* A solution of **16** (138.9 mg, 0.252 mmol), benzene (25 mL), and Et_2O (0.2 mL) was cooled to 5 °C in an ice and water bath. A solution of *t*-butyllithium in hexanes (1.46 M, 0.39 mL, 0.57 mmol) was added dropwise, and the solution and was stirred for 3 min. A solution of $MesB(OMe)_2$ in Et_2O (0.31 M, 0.90 mL, 0.28 mmol) was added dropwise by syringe to the reaction vessel. The reaction mixture was allowed to slowly warm to room temperature over 19 h. The reaction mixture was diluted with 5% NH_4Cl, and the aqueous layer was extracted with hexane (3×). The combined organic layers were washed with brine, dried over anhydrous $MgSO_4$, filtered, and concentrated under reduced pressure. The crude solid was further purified by column chromatography (SiO_2:hexane) to yield **17** as a yellow solid (92.9 mg, 0.178 mmol, 71%) with trace alkyl impurities. ^{1}H NMR (400 MHz, CD_2Cl_2) δ: 8.69 (dd, 1H, J = 0.8, 8.8 Hz), 8.11 (d, 1H, J = 8.6 Hz), 7.88 (m, 2H), 7.84 (dd, 1H, J = 0.8, 12 Hz), 7.55 (d, 1H, J = 12 Hz), 7.46 (m, 2H), 7.19 (m, 1H), 6.87 (d, 2H, J = 0.6 Hz), 2.36 (s, 3H), 1.86 (s, 6H), 1.27 (sept, 3H, J = 7.6 Hz), 1.07 (d, 18H, J = 7.3 Hz). ^{13}C {^{1}H} NMR (100 MHz, $CDCl_3$) δ: 159.2, 149.4, 144.9, 139.9, 136.4, 136.4, 136.0, 135.9, 133.2, 133.1, 132.8, 132.5, 130.4, 127.9, 127.7, 127.6, 126.4, 125.9, 125.4, 23.1, 21.4, 18.7, 12.0. HRMS (EI) found m/z = 520.2799 (M^+), calculated for $C_{34}H_{41}BSSi$: 520.2791.

*12-Mesitylnaphtho[2′,1′:6,7]borepino[3,2-b]thiophene (**7**).* Trifluoroacetic acid (1.2 mL) was added in 3 portions over 3 h to a solution of **17** (80.7 mg, 0.155 mmol) in CH_2Cl_2 (20 mL) under a N_2 atmosphere. The solution was stirred for 2 h in the absence of light, and the reaction was monitored by TLC. The reaction mixture was diluted with water and extracted with $CHCl_3$ (3×). The combined organic layers were washed with brine, dried over anhydrous $MgSO_4$, filtered, and concentrated under reduced pressure. The crude solid was further purified by column chromatography (SiO_2:hexane) to yield **7** as a pure yellow solid (48.2 mg, 0.132 mmol, 85%). ^{1}H NMR (400 MHz, CD_2Cl_2) δ: 8.60 (dd, 1H, J = 0.7, 8.8 Hz), 8.12 (d, 1H, 8.8 Hz), 7.88 (d, 1H, J = 8.9 Hz), 7.80 (dd, 1H, J = 0.6, 12 Hz), 7.58 (d, 1H, J = 12 Hz), 7.47 (m, 2H), 7.33 (dd, 1H, J = 0.7, 5.2), 7.19 (m, 1H), 6.89 (d, 2H, 0.6 Hz), 2.37 (s, 3H), 1.87 (s, 6H). ^{13}C {^{1}H} NMR (100 MHz, CD_2Cl_2) δ: 155.4, 144.8, 139.7, 136.7, 136.6, 133.5, 133.2, 133.1, 133.0, 130.7, 128.2, 128.0, 127.2, 126.8, 126.5, 126.0, 125.9, 23.2, 21.4. HRMS (EI) found m/z = 364.1455 (M^+), calculated for $C_{25}H_{21}BS$: 364.1457.

*(((2,5-Dibromo-1,4-phenylene)bis(ethyne-2,1-diyl))bis(4-bromothiophene-5,2-diyl))bis(triisopropylsilane) (**18**).* A 1:3 diisopropylamine:toluene mixture was degassed in a dry 250 mL, 3-neck, round-bottom flask prior to use. A 250 mL Schlenk flask was charged with 1,4-dibromo-2,5-diiodobenzene (2.19 g, 4.48 mmol), $Pd(PPh_3)_4$ (14.5 g, 0.207 mmol), and CuI (83.6 mg, 0.439 mmol). The mixed solvent (90 mL) was added to the flask. **10** (3.02 g, 8.80 mmol) was dissolved in a dry round-bottom flask with degassed toluene (30 mL) and was transferred dropwise by cannula to the Schlenk flask. The reaction mixture was stirred at 60 °C for 20 h and was allowed to cool to room temperature. A 5% NH_4Cl solution was added and extracted against $CHCl_3$ (3×). The combined organic layers were washed with brine, dried over anhydrous $MgSO_4$, and concentrated under reduced pressure to provide a brown solid that was further purified by column chromatography (SiO_2:hexane) to yield **18** as a pure yellow solid (3.14 g, 3.42 mmol, 76%). ^{1}H NMR (400 MHz, $CDCl_3$) δ: 7.79 (s, 2H), 7.12 (s, 2H), 7.33 (sept, 6H, J = 7.4 Hz), 1.11 (d, 36 H, J = 7.4 Hz).

DOI: 10.1021/acs.joc.6b00927
J. Org. Chem. 2016, 81, 5595−5605

^{13}C {^{1}H} NMR (100 MHz, $CDCl_3$) δ: 140.3, 137.9, 136.1, 126.4, 124.6, 123.9, 118.4, 95.2, 88.7, 18.6, 11.8. HRMS (EI): found m/z = 914.9450 (M^+), calculated for $C_{36}H_{46}Br_4S_2Si_2$: 914.9391.

*(((1Z,1′Z)-(2,5-Dibromo-1,4-phenylene)bis(ethene-2,1-diyl))bis(4-bromothiophene-5,2-diyl))bis(triisopropylsilane) (**19**).* A solution of **18** (2.67 g, 2.91 mmol), titanium isopropoxide (5.35 g, 18.8 mmol) in toluene (180 mL) was set to stir in a 250 mL Schlenk tube. A solution of *i*-propylmagnesium chloride in Et_2O (1.71 M, 28.0 mL, 47.9 mmol) was added in a single portion, and the reaction was stirred for 30 min at −78 °C in an acetone and dry ice bath and then warmed to −40 °C in an acetonitrile and dry ice bath for 3 h. Water (11 mL) was added to the cooled solution, which was then allowed to warm to room temperature over 18 h. The reaction mixture was diluted with 1 M HCl and extracted with EtOAc (3×), and the combined organic layers were washed with brine, dried over anhydrous $MgSO_4$, filtered, and concentrated under reduced pressure. The crude solid was further purified by a short chromatographic plug (SiO_2:hexane) to yield a yellow solid that was triturated with Et_2O (2×) to give **19** (2.25 mg, 2.44 mmol, 84%). ^{1}H NMR (400 MHz, $CDCl_3$) δ: 7.70 (s, 2H), 7.04 (s, 2H), 6.84 (d, 2H, J = 12 Hz), 6.56 (d, 2H, J = 12 Hz), 1.22 (sept, 6H, J = 7.3 Hz), 1.04 (d, 38H, J = 7.3 Hz). ^{13}C {^{1}H} NMR (100 MHz, $CDCl_3$) δ: 138.1, 137.7, 137.4, 136.3, 134.9, 128.5, 123.6, 122.4, 114.7, 18.6, 11.7. HRMS (EI) found m/z = 917.9614 (M^+), calculated for $C_{36}H_{50}Br_4S_2Si_2$: 917.9626.

*2,9-Bistriisopropylsilyl-4,11-dimesitylbenzo[1″,2″:6,7;4″,5″:6′,7′]diborepino[3,2-b:3′,2′-b′]dithiophene (**20**).* A solution of **19** (122 mg, 0.133 mmol), benzene (20 mL), and Et_2O (1.0 mL) was cooled to 5 °C in an ice and water bath. A solution of *t*-butyllithium in hexanes (1.48 M, 0.72 mL, 1.1 mmol) was added dropwise, and the solution and was stirred for 5 min. A solution of $MesB(OMe)_2$ in Et_2O (0.31 M, 0.90 mL, 0.28 mmol) was added dropwise by syringe to the reaction vessel. The reaction mixture was allowed to slowly warm to room temperature over 19 h. The reaction mixture was diluted with water, and the aqueous layer was extracted with $CHCl_3$ (5×). The combined organic layers were washed with brine, dried over anhydrous $MgSO_4$, filtered, and concentrated under reduced pressure. The crude solid was further purified by column chromatography (SiO_2:hexane, 10% $CHCl_3$) to yield the yellow solid **20** (78.3 mg, 0.0907 mmol, 68%) as a pure compound. ^{1}H NMR (400 MHz, $CDCl_3$) δ: 8.63 (s, 2H), 7.58 (d, 2H, J = 12 Hz), 7.41 (s, 2H), 7.36 (d, 2H, J = 12 Hz), 6.94 (s, 4H), 2.45 (s, 6H), 1.95 (s, 12H), 1.28 (sept, 6H, J = 7.4 Hz), 1.05 (d, 38H, J = 7.4 Hz). ^{13}C {^{1}H} NMR (100 MHz, $CDCl_3$) δ: 161.5, 148.40, 148.38, 141.8, 137.9, 136.3, 135.9, 133.2, 127.1, 123.5, 27.1, 23.1, 18.6, 11.9. HRMS (FAB) found m/z = 862.4797 (M^+), calculated for $C_{54}H_{72}B_2S_2Si_2$: 862.4800.

*4,11-Dimesitylbenzo[1″,2″:6,7;4″,5″:6′,7′]diborepino[3,2-b:3′,2′-b′]dithiophene (**8**).* Trifluoroacetic acid (2 mL) was added in a single portion to a solution of **20** (82.1 mg, 0.0951 mmol) in CH_2Cl_2 (40 mL) under a N_2 atmosphere. The solution was stirred for 21 h in the absence of light. The reaction mixture was diluted with water and extracted with $CHCl_3$ (3×). The combined organic layers were washed with brine, dried over anhydrous $MgSO_4$, filtered, and concentrated under reduced pressure. The crude solid was further purified by column chromatography (SiO_2:hexane, 10% $CHCl_3$) to yield **8** as a yellow solid (37.9 mg, 0.0689 mmol, 73%). ^{1}H NMR (400 MHz, CD_2Cl_2) δ: 8.65 (s, 2H), 7.58 (d, 2H, J = 12 Hz), 7.43 (d, 2H, J = 5.2 Hz), 7.39 (d, 2H, J = 12 Hz), 7.27 (d, 2H, J = 5.2 Hz), 6.98 (s, 4H), 2.43 (s, 6H), 1.94 (s, 12 H). HRMS (EI) found m/z = 550.2131 (M^+), calculated for $C_{36}H_{32}B_2S_2$: 550.2132.

*1,5-Dibromonaphthalene-2,6-diyl Bis(trifluoromethanesulfonate) (**21**).* A 25 mL Schlenk flask was charged with 1,5-dibromonaphthalene-2,6-diol (202 mg, 0.632 mmol), DCM (6 mL), and a stir bar under N_2. Pyridine (0.3 mL) was added, and the solution was cooled to 0 °C in an ice and water bath. Trifluoromethanesulfonic anhydride (0.27 mL, 1.6 mmol) was added dropwise, and mixture was allowed to stir for 18 h and warm up to room temperature. The reaction mixture was diluted with 1 M HCl and extracted with $CHCl_3$ (3×). The combined organic layers were dried with $MgSO_4$ and filtered, and the solvent was removed under reduced pressure to provide a brown solid that was further purified by a short chromatographic plug (SiO_2: 80% hexane, 20% EtOAc) to yield **21** as a pure white solid (267 mg, 0.459 mmol, 73%). ^{1}H NMR (400 MHz, $CDCl_3$) δ: 8.47 (d, 2H, 9.2 Hz), 7.65 (d, 2H, 9.2 Hz). ^{13}C {^{1}H} NMR (100 MHz, $CDCl_3$) δ: 146.6, 132.6, 130.0, 122.9, 116.8. HRMS (EI): found m/z = 579.7696 (M^+), calculated for $C_{12}H_4Br_2F_6O_6S_2$: 579.7720.

*(((1,5-Dibromonaphthalene-2,6-diyl)bis(ethyne-2,1-diyl))bis(4-bromothiophene-5,2-diyl))bis(triisopropylsilane) (**22**).* A 100 mL Schlenk flask was charged with $Pd(PPh_3)_4$ (229 mg, 0.198 mmol), CuI (61.7 mg, 0.324 mmol), **21** (572 mg, 0.982 mmol), and a stir bar. Dimethylformamide (40 mL) and diisopropylamine (10 mL) were added, and the mixture was stirred at room temperature. A solution of **10** (836 mg, 2.44 mmol) in diisopropylamine (10 mL) was transferred by cannula to the reaction mixture over 30 min and stirred for 17 h. The reaction was diluted with a 1 M HCl solution, and the aqueous layer was extracted against hexane (3×). The combined organic layers were washed with a saturated solution of 5% NH_4Cl, dried with $MgSO_4$, and filtered, and the solvent was removed under reduced pressure. The crude product was further purified with a chromatographic column (SiO_2:hexane) to afford **22** as a pure yellow solid (211 mg, 0.218 mmol, 22%). ^{1}H NMR (400 MHz, $CDCl_3$) δ: 8.30 (d, 2H, J = 8.6 Hz), 7.70 (d, 2H, J = 8.6 Hz), 7.14 (s, 2H), 1.33 (sept, 6H, J = 7.2 Hz), 1.12 (d, 36H, J = 7.4 Hz). ^{13}C {^{1}H} NMR (100 MHz, $CDCl_3$) δ: 140.0, 137.9, 132.6, 130.7, 127.6, 126.1, 125.0, 124.8, 118.2, 97.3, 88.1, 18.6, 11.8. HRMS (EI) found m/z = 963.9413 (M^+), calculated for $C_{40}H_{48}Br_4S_2Si_2$: 963.9469.

*(((1Z,1′Z)-(1,5-Dibromonaphthalene-2,6-diyl)bis(ethene-2,1-diyl))bis(4-bromothiophene-5,2-diyl))bis(triisopropylsilane) (**23**).* A solution of **22** (211 mg, 0.218 mmol), titanium isopropoxide (0.30 mL, 1.0 mmol) in toluene (25 mL) was set to stir in a 100 mL Schlenk tube. A solution of *i*-propylmagnesium chloride in Et_2O (2.00 M, 1.1 mL, 2.2 mmol) was added in a single portion, and the reaction was stirred for 30 min at −78 °C in an acetone and dry ice bath and then warmed to −45 °C in an acetonitrile and dry ice bath for 3 h. Water (1 mL) was added to the cooled solution, which was then allowed to slowly warm to room temperature over 19 h. The reaction mixture was diluted with 1 M HCl and hexane, the aqueous layer was extracted against hexane (3×), and the combined organic layers were washed with brine, dried over anhydrous $MgSO_4$, filtered, and concentrated under reduced pressure. The crude solid was further purified by a short chromatographic plug (SiO_2:hexane) to yield **23** as a yellow solid (203 mg, 0.209 mmol, 96%) with trace alkyl impurities. ^{1}H NMR (400 MHz, $CDCl_3$) δ: 8.19 (d, 2H, J = 8.6 Hz), 7.49 (d, 2H, J = 8.7 Hz), 7.02 (s, 2H), 6.93 (d, 2H, J = 12 Hz), 6.88 (d, 2H, J = 12 Hz), 1.12 (sept, 6H, J = 7.0 Hz), 0.96 (d, 36H, J = 7.2 Hz). ^{13}C {^{1}H} NMR (100 MHz, $CDCl_3$) δ: 138.2, 137.2, 136.4, 136.3, 133.2, 130.8, 129.5, 126.8, 124.3, 123.3, 113.9, 18.5, 11.6. LRMS (EI) found m/z = 967.9672 (M^+), calculated for $C_{40}H_{52}Br_4S_2Si_2$: 967.9782.

*2,10-Bistriisopropylsilyl-4,12-dimesitylnaphtho[1″,2″:7,6;6″,7″:6′,7′]diborepino[3,2-b:3′,2′-b′]dithiophene (**24**).* A solution of **23** (212 mg, 0.218 mmol), benzene (50 mL), and Et_2O (1.0 mL) was cooled to 5 °C in an ice and water bath. A solution of *t*-butyllithium in hexanes (1.70 M, 1.00 mL, 1.70 mmol) was added dropwise to the solution and was allowed to stir for 2 min. A solution of $MesB(OMe)_2$ in Et_2O (0.52 M, 0.90 mL, 0.47 mmol) was added dropwise by syringe to the reaction vessel. The reaction mixture was allowed to slowly warm to room temperature over 19 h. The reaction mixture was diluted with 5% NH_4Cl, and the aqueous layer was extracted with EtOAc (5×). The combined organic layers were washed with brine, dried over anhydrous $MgSO_4$, filtered, and concentrated under reduced pressure. The crude solid was further purified by column chromatography (SiO_2:hexane, 1% $CHCl_3$) to yield **24** as a yellow solid (62.7 mg, 0.0687 mmol, 31%) with trace alkyl impurities. ^{1}H NMR (400 MHz, CD_2Cl_2) δ: 8.72 (d, 2H, J = 8.8 Hz), 7.80 (dd, 2H, J = 0.7, 12 Hz), 7.45 (m, 6H), 6.84 (d, 4H, J = 0.6 Hz), 2.34 (s, 6H), 1.83 (s, 12H), 1.28 (sept, 6H, J = 7.2 Hz), 1.06 (d, 36H, J = 7.3 Hz). ^{13}C {^{1}H} NMR (100 MHz, CD_2Cl_2) δ: 159.9, 159.4, 144.6, 140.7, 137.0, 136.8, 136.5, 135.3, 132.0, 131.0, 127.8, 125.8, 105.4, 23.3, 21.3, 18.7, 12.3. HRMS (EI) found m/z = 912.4980 (M^+), calculated for $C_{58}H_{74}B_2S_2Si_2$: 912.4957.

DOI: 10.1021/acs.joc.6b00927
J. Org. Chem. 2016, 81, 5595−5605

*4,12-Dimesitylnaphtho[1″,2″:7,6;6″,7″:6′,7′]diborepino[3,2-b:3′,2′-b′]dithiophene (**9**).* Trifluoroacetic acid (0.5 mL) was added in 2 portions over 2 h to a solution of **24** (62.7 mg, 0.0687 mmol) in CH_2Cl_2 (10 mL) under a N_2 atmosphere. The solution was stirred in the absence of light and monitored by TLC. The reaction mixture was diluted with water and extracted with $CHCl_3$ (3×). The combined organic layers were washed with brine, dried over anhydrous $MgSO_4$, filtered, and concentrated under reduced pressure. The crude solid was further purified by column chromatography (SiO_2:hexane, 5% $CHCl_3$) to yield **9** as a pure yellow solid (15.7 mg, 0.0261 mmol, 38%). ^{1}H NMR (400 MHz, CD Cl_3) δ: 8.64 (d, 2H, 8.8 Hz), 7.73 (d, 2H, 12 Hz), 7.43 (m, 4H), 7.39 (d, 2H, J = 5.3 Hz), 7.28 (dd, 2H, J = 0.7, 5.2 Hz), 6.82 (d, 4H, J = 0.6 Hz), 2.35 (s, 6H), 1.82 (s, 12H). ^{13}C {^{1}H} NMR (100 MHz, $CDCl_3$) δ: 155.3, 144.5, 139.8, 136.8, 136.3, 135.0, 132.4, 130.8, 127.8, 126.0, 125.9, 23.2, 21.4. HRMS (EI) found m/z = 600.2301 (M^+), calculated for $C_{40}H_{34}B_2S_2$: 600.2288.

■ ASSOCIATED CONTENT

Supporting Information

The Supporting Information is available free of charge on the ACS Publications website at DOI: 10.1021/acs.joc.6b00927.

Copies of ^{1}H NMR, ^{13}C NMR; cyclic voltammetry of **6**, **7**, **8**, and **9**; DFT calculated Cartesian coordinates for **1**−**9**; tabulated photophysical data, proposed nomenclature, details on the borepin formation step, calculated and observed ^{1}H NMR assignments, and long-term stability studies (PDF)

Crystallographic information for **6** (CCDC: 1475804) (CIF)

Crystallographic information for **7** (CCDC: 1475807) (CIF)

Crystallographic information for **8** (CCDC: 1475803) (CIF)

Crystallographic information for **9** (CCDC: 1475805) (CIF)

Crystallographic information for **20** (CCDC: 1475806) (CIF)

■ AUTHOR INFORMATION

Corresponding Author

*E-mail: tovar@jhu.edu.

Notes

The authors declare no competing financial interest.

■ ACKNOWLEDGMENTS

The authors would like thank Eric Chan for his early synthetic contributions. This work was supported by Johns Hopkins University, the National Science Foundation (CHE-1464798), and the Achievement Rewards for College Scholars Foundation (fellowship for R.E.M.).

■ REFERENCES

(1) Messersmith, R. E.; Tovar, J. D. *J. Phys. Org. Chem.* **2015**, *28*, 378−387.

(2) Ashe, A. J.; Klein, W.; Rousseau, R. *Organometallics* **1993**, *12*, 3225−3231.

(3) Iida, A.; Saito, S.; Sasamori, T.; Yamaguchi, S. *Angew. Chem., Int. Ed.* **2013**, *52*, 3760−3764.

(4) Braunschweig, H.; Damme, A.; Jimenez-Halla, J. O. C.; Hörl, C.; Krummenacher, I.; Kupfer, T.; Mailänder, L.; Radacki, K. *J. Am. Chem. Soc.* **2012**, *134*, 20169−20177.

(5) Entwistle, C. D.; Marder, T. B. *Chem. Mater.* **2004**, *16*, 4574−4585.

(6) Subramanian, G.; Schleyer, P. v. R.; Jiao, H. *Organometallics* **1997**, *16*, 2362−2369.

(7) Schulman, J. M.; Disch, R. L. *Organometallics* **2000**, *19*, 2932−2936.

(8) Ashe, A. J.; Kampf, J. W.; Kausch, C. M.; Konishi, H.; Kristen, M. O.; Kroker, J. *Organometallics* **1990**, *9*, 2944−2948.

(9) Levine, D. R.; Siegler, M. A.; Tovar, J. D. *J. Am. Chem. Soc.* **2014**, *136*, 7132−7139.

(10) Jeffries, A. T., III; Gronowitz, S. *Chem. Scr.* **1973**, *4*, 183−187.

(11) Saito, S.; Matsuo, K.; Yamaguchi, S. *J. Am. Chem. Soc.* **2012**, *134*, 9130−9133.

(12) Mercier, L. G.; Piers, W. E.; Parvez, M. *Angew. Chem., Int. Ed.* **2009**, *48*, 6108−6111.

(13) Caruso, A.; Siegler, M. A.; Tovar, J. D. *Angew. Chem., Int. Ed.* **2010**, *49*, 4213−4217.

(14) Caruso, A.; Tovar, J. D. *Org. Lett.* **2011**, *13*, 3106−3109.

(15) Levine, D. R.; Caruso, A.; Siegler, M. A.; Tovar, J. D. *Chem. Commun.* **2012**, *48*, 6256−6258.

(16) Caruso, A.; Tovar, J. D. *J. Org. Chem.* **2011**, *76*, 2227−2239.

(17) Anthony, J. E. *Nat. Mater.* **2014**, *13*, 773−775.

(18) Anthony, J. E. *Angew. Chem., Int. Ed.* **2008**, *47*, 452−483.

(19) Gronowitz, S.; Gassne, P.; Yom-Tov, B. *Acta Chem. Scand.* **1969**, *23*, 2927−2930.

(20) van Tamelen, E. E.; Brieger, G.; Untch, K. G. *Tetrahedron Lett.* **1960**, *1*, 14−15.

(21) Jäkle, F. *Coord. Chem. Rev.* **2006**, *250*, 1107−1121.

(22) Jäkle, F. *Chem. Rev.* **2010**, *110*, 3985−4022.

(23) Tang, M. L.; Reichardt, A. D.; Wei, P.; Bao, Z. *J. Am. Chem. Soc.* **2009**, *131*, 5264−5273.

(24) Nakano, M.; Niimi, K.; Miyazaki, E.; Osaka, I.; Takimiya, K. *J. Org. Chem.* **2012**, *77*, 8099−8111.

(25) Baker, R.; Eaborn, C.; Taylor, R. *J. Chem. Soc., Perkin Trans. 2* **1972**, 97−101.

(26) Mitchell, R. H. *Chem. Rev.* **2001**, *101*, 1301−1316.

(27) Mitchell, R. H.; Iyer, V. S.; Khalifa, N.; Mahadevan, R.; Venugopalan, S.; Weerawarna, S. A.; Zhou, P. *J. Am. Chem. Soc.* **1995**, *117*, 1514−1532.

(28) Fukazawa, A.; Yamada, H.; Sasaki, Y.; Akiyama, S.; Yamaguchi, S. *Chem.—Asian J.* **2010**, *5*, 466−469.

(29) Moslin, R. M.; Espino, C. G.; Swager, T. M. *Macromolecules* **2009**, *42*, 452−454.

(30) Levine, D. R. Engineering electronic diversity and synthetic versatility into borepin-based π-conjugated organoboron materials. Ph.D. Thesis, Johns Hopkins University, Baltimore, MD, 2016.

(31) Bailey, W. F.; Luderer, M. R.; Jordan, K. P. *J. Org. Chem.* **2006**, *71*, 2825−2828.

(32) Bailey, W. F.; Brubaker, J. D.; Jordan, K. P. *J. Organomet. Chem.* **2003**, *681*, 210−214.

(33) Shono, K.; Sumino, Y.; Tanaka, S.; Tamba, S.; Mori, A. *Org. Chem. Front.* **2014**, *1*, 678−682.

(34) Zhang, X.; Côté, A. P.; Matzger, A. J. *J. Am. Chem. Soc.* **2005**, *127*, 10502−10503.

(35) Gomes, J. A. N. F.; Mallion, R. B. *Chem. Rev.* **2001**, *101*, 1349−1384.

(36) Krygowski, T. M.; Cyrański, M. K.; Czarnocki, Z.; Häfelinger, G.; Katritzky, A. R. *Tetrahedron* **2000**, *56*, 1783−1796.

(37) Cyrański, M. K. *Chem. Rev.* **2005**, *105*, 3773−3811.

(38) Cyrański, M. K.; Schleyer, P. v. R.; Krygowski, T. M.; Jiao, H.; Hohlneicher, G. *Tetrahedron* **2003**, *59*, 1657−1665.

(39) Krygowski, T. M.; Cyrański, M. K. *Chem. Rev.* **2001**, *101*, 1385−1420.

(40) Gershoni-Poranne, R.; Stanger, A. *Chem. Soc. Rev.* **2015**, *44*, 6597−6615.

(41) Cyrański, M. K.; Krygowski, T. M.; Katritzky, A. R.; Schleyer, P. v. R. *J. Org. Chem.* **2002**, *67*, 1333−1338.

(42) Katritzky, A. R.; Jug, K.; Oniciu, D. C. *Chem. Rev.* **2001**, *101*, 1421−1450.

(43) Yuan, Z.; Collings, J. C.; Taylor, N. J.; Marder, T. B.; Jardin, C.; Halet, J.-F. *J. Solid State Chem.* **2000**, *154*, 5−12.

DOI: 10.1021/acs.joc.6b00927
J. Org. Chem. 2016, 81, 5595−5605

(44) Wiberg, K. B. *J. Org. Chem.* **1997**, *62*, 5720−5727.
(45) Cyrański, M. K.; Stepień, B. T.; Krygowski, T. M. *Tetrahedron* **2000**, *56*, 9663−9667.
(46) Zhang, L.; Cao, Y.; Colella, N. S.; Liang, Y.; Brédas, J.-L.; Houk, K. N.; Briseno, A. L. *Acc. Chem. Res.* **2015**, *48*, 500−509.
(47) Desiraju, G. R.; Gavezzotti, A. *J. Chem. Soc., Chem. Commun.* **1989**, 621−623.
(48) Kruszewski, J.; Krygowski, T. M. *Tetrahedron Lett.* **1972**, *13*, 3839−3842.
(49) Chen, Z.; Wannere, C. S.; Corminboeuf, C.; Puchta, R.; Schleyer, P. v. R. *Chem. Rev.* **2005**, *105*, 3842−3888.
(50) Schleyer, P. v. R.; Maerker, C.; Dransfeld, A.; Jiao, H.; Hommes, N. J. R. v. E. *J. Am. Chem. Soc.* **1996**, *118*, 6317−6318.
(51) Feixas, F.; Matito, E.; Poater, J.; Sola, M. *Chem. Soc. Rev.* **2015**, *44*, 6434−6451.
(52) Cao, J.; London, G.; Dumele, O.; von Wantoch Rekowski, M.; Trapp, N.; Ruhlmann, L.; Boudon, C.; Stanger, A.; Diederich, F. *J. Am. Chem. Soc.* **2015**, *137*, 7178−7188.
(53) Wu, J. I.; Wannere, C. S.; Mo, Y.; Schleyer, P. v. R.; Bunz, U. H. F. *J. Org. Chem.* **2009**, *74*, 4343−4349.
(54) Pierrefixe, S. C. A. H.; Bickelhaupt, F. M. *Chem.—Eur. J.* **2007**, *13*, 6321−6328.
(55) Krygowski, T. M. *J. Chem. Inf. Comput. Sci.* **1993**, *33*, 70−78.
(56) Shaik, S. S.; Hiberty, P. C. *J. Am. Chem. Soc.* **1985**, *107*, 3089−3095.
(57) Mercier, L. G. Design, synthesis and characterization of fluorescent organoboron and organosilicon compounds. Ph.D. Thesis, University of Calgary, Calgary, AB, Canada, 2011.
(58) Pelter, A.; Smith, K.; Buss, D.; Jin, Z. *Heteroat. Chem.* **1992**, *3*, 275−277.
(59) He, M.; Hu, J.; Niu, W.; Tandia, A. Novel fused naphthalene cyclohetero ring compounds, and methods and uses thereof. PCT/US2013/034347.
(60) Frisch, M. J.; Trucks, G. W.; Schlegel, H. B.; Scuseria, G. E.; Robb, M. A.; Cheeseman, J. R.; Scalmani, G.; Barone, V.; Mennucci, B.; Petersson, G. A.; Nakatsuji, H.; Caricato, M.; Li, X.; Hratchian, H. P.; Izmaylov, A. F.; Bloino, J.; Zheng, G.; Sonnenberg, J. L.; Hada, M.; Ehara, M.; Toyota, K.; Fukuda, R.; Hasegawa, J.; Ishida, M.; Nakajima, T.; Honda, Y.; Kitao, O.; Nakai, H.; Vreven, T.; Montgomery, J. A., Jr.; Peralta, J. E.; Ogliaro, F.; Bearpark, M.; Heyd, J. J.; Brothers, E.; Kudin, K. N.; Staroverov, V. N.; Kobayashi, R.; Normand, J.; Raghavachari, K.; Rendell, A.; Burant, J. C.; Iyengar, S. S.; Tomasi, J.; Cossi, M.; Rega, N.; Millam, J. M.; Klene, M.; Knox, J. E.; Cross, J. B.; Bakken, V.; Adamo, C.; Jaramillo, J.; Gomperts, R.; Stratmann, R. E.; Yazyev, O.; Austin, A. J.; Cammi, R.; Pomelli, C.; Ochterski, J. W.; Martin, R. L.; Morokuma, K.; Zakrzewski, V. G.; Voth, G. A.; Salvador, P.; Dannenberg, J. J.; Dapprich, S.; Daniels, A. D.; Farkas, Ö.; Foresman, J. B.; Ortiz, J. V.; Cioslowski, J.; Fox, D. J. *Gaussian 09*; Gaussian, Inc.: Wallingford, CT, 2009.

DOI: 10.1021/acs.joc.6b00927
J. Org. Chem. 2016, 81, 5595−5605